IMS 2015
12th International Mathematica Symposium

Scroll Compressor

Fluid mechanical modeling

M. Wannassi
Department Mechanics and Glasses
Institut de Physique de Rennes
UMR 6251- CNRS/University of Rennes 1

M. Buisson
Department Mechanics and Glasses
Institut de Physique de Rennes
UMR 6251- CNRS/University of Rennes 1

Abstract

We adopt the modelization of Blunier and all (2009) based on a geometrical description of the scroll wraps in order to study scroll compressor. A precise geometry is necessary because this is the main factors which affects the efficiency of the compressor and this is the basis to establish an accurate thermodynamic model. With *Mathematica*, this paper uses this novel description of the geometry based on the parametric equations for the circle involutes in a novel reference system, in order to exploit the symmetry of the compressor: we obtain exact analytical expressions of the compression and discharge chamber volumes, together with all the geometrical parameters. Such formal calculus allowes the compressor to be optimized geometrically and to investigates a lot of others geometries. We can also analytically observe the conjugacy points, describe the compression process in detail and estimate the chamber volumes . The gap between scroll due to manufacturing and wear is analyzed because this determines the leakage between neighboring chambers in the compressor. Description of the chambers and of the leakage give us a set of ordinary coupled differential equations for the temperature and pressure which represent the kinematic of the scroll associated with the thermodynamic evolutions of air or refrigerant .

Introduction

The scroll compressor was originally invented by Leon Creux (1905) to compress air or refrigerant. This machine has been put into commercial use since the early 1980's. The manufacturing consists of two nested identical scrolls whose axes of rotation do not meet each other so that one scroll is rotated through 180° with respect to the other; they are assembled in the way that they can touch themselves at different points and form a series of successive chambers. The advantages of this concept is:

-the small number of moving parts

-a high efficiency

-a low level of noise and vibrations.

However the main problem is that manufacturing must be precise to respect the design of the scroll profile which plays a key role in the performances.

In the litterature, we can find a lot of geometric shapes of scroll, involute angles, general expressions of all chamber volumes, correction term for the suction chamber, kinds of leakage (flank and radial), thermodynamic analysis, (Yanagisawa et al. (1990), Halm (1997), Chen et al. (2002), Lee and Wu (1995) and Hirano et al. (1990); analytical description of the compression and discharge chamber volumes (Morishita et al. (1984)), (Nieter, 1988), (Nieter and Gagne, 1992). Liu et al. (1992) propose a graphical method and Lee and Wu (1995) give an analytical method in order to have a perfect meshing profile (i.e., zero clearance volume) and to optimize the discharge process.

Wang et al. (2005) noted the limitation of fixed initial involute angles in Halm and Chen, and developed a model with discretionary initial angles of involute. Then a major breakthrough came with Gravensen et al. (1998); in Gravensen and Henriksen (2001) the entire geometry of the spiral is redefined with two planar curves where the involute is a special case: they give access to the analysis of variable-wall-thickness scrolls. The work of Blunier (2006) and Blunier (2009) uses Gravesen's analysis in order to introduce an original way to describe the geometry of the scroll wraps in which the symmetries are easily exploited to establish a thermodynamic model of the scroll compressor. The flank and radial leakages are taken into account and the discharge process is not considered as symmetrical.

In this communication, we use *Mathematica* :

- to describe the geometry, based on the idea of Gravensen (Gravensen and Henriksen, 2001) and Blunier (2006),

-to adopt the novel reference frame of these authors in order to exploit the symmetry of the two scrolls.

-to present the development of a comprehensive scroll model, using a set of function developed analytically and which includes models for the compression process.

This analytical approach reveals the ability of *Mathematica* to successfully manage the complicated geometries.

Analytical analysis of scroll compressor geometry (see Blunier and all (2006)for more details)

The shape of the investigated scroll is described by an involute of circle in a general frame. The fixed and orbiting scrolls are therefore defined as two involutes that develop around a common basic circle with radius r_b and are offset by a constant distance. This framework makes all the properties of the scroll appear very clearly. Each involute is defined by introducing the orthonormal frame (t, n):

$$t[\varphi\_] := \{\text{Cos}[\varphi], \text{Sin}[\varphi]\};$$
$$n[\varphi\_] := \{-\text{Sin}[\varphi], \text{Cos}[\varphi]\};$$
(1)

Where t[φ_] is the unit tangent vector and n[φ_] the unit normal vector.
The involute of a circle is given by:

$$S_{xy}[\varphi\_] := r_b\, t[\varphi] - r_b\,(\varphi - \varphi_{y0})\, n[\varphi] + \xi$$
(2)

Where r_b is the involute basic circle radius, φ is the involute angle, φ_{y0} the internal or external involute initial angle on the base circle with x∈{f,m} and y∈{i,e}.

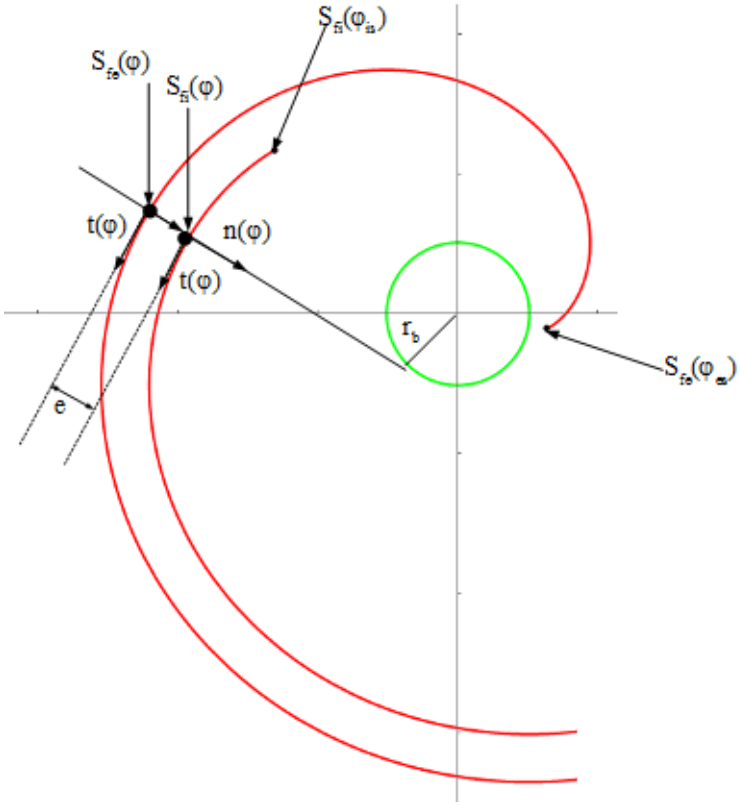

Fig1. Scroll geometry

Fixed spiral geometry

The representation of the fixed (f) scroll can be determined as follows:

$$S_{fe}[r_b\_, \varphi_{e0}\_, \varphi\_] := r_b * (t[\varphi] - (\varphi - \varphi_{e0}) * n[\varphi])$$
(3)

$$S_{fi}[r_b\_, \varphi_{i0}\_, \varphi\_] := r_b * (t[\varphi] - (\varphi - \varphi_{i0}) * n[\varphi])$$
(4)

where S_{fe} and S_{fi} are, respectively, the external (e) and internal (i) involutes. The angles φ_{es} and φ_{is} are the external and internal starting angles,φ_{max} the involute ending angle, φ_{e0} and φ_{i0} the initial angles of the external and internal involutes. The domains of definition of the internal and external involutes are, respectively, $I_e = [\varphi_{es}, \varphi_{max}]$ and $I_i = [\varphi_{is}, \varphi_{max}]$.

Interpolating circle

In order to complete the scroll shape representation, $S_{fi}(\varphi_{is})$ and $S_{fe}(\varphi_{es})$ have to be connected. For the investigated compressor the extended part can be described by an arc of a circle. The circle is represented by:

$$C_{cf}[r_b\_, r_c\_, \varphi_{i0}\_, \varphi_{is}\_, \alpha\_] := o_{cf}[r_b, r_c, \varphi_{i0}, \varphi_{is}] - r_c * n[\alpha] \tag{5}$$

where $o_{c,f}$ and r_c are, respectively, the centre and the radius of the circle. With:

$$r_c := \frac{r_b * (2 + \xi_1^2 + \xi_2^2 - (2 + 2(\xi_1 * \xi_2))\,\text{Cos}[\xi_3] - 2(\xi_2 - \xi_1)\,\text{Sin}[\xi_3])}{(2(\xi_2 - \xi_1\ \text{Cos}[\xi_3] - \text{Sin}[\xi_3]))} \tag{6}$$

Where: $\xi_1 := \varphi_{es} - \varphi_{e0}$; $\xi_2 := \varphi_{is} - \varphi_{i0}$; $\xi_3 := \varphi_{is} - \varphi_{es}$; and,

$$o_{c,f}[r_b\_, r_c\_, \varphi_{i0}\_, \varphi_{is}\_] := r_b * t[\varphi_{is}] + (r_c - r_b * (\varphi_{is} - \varphi_{i0})) * n[\varphi_{is}] \tag{7}$$

The domain of definition I_c of the interpolating circle is the following:

$$I_c = [\varphi_{is} - \Delta\alpha, \varphi_{is}] \tag{8}$$

$$\Delta\alpha := \text{ArcCos}\left[1 - \frac{r_b}{r_c} * (\xi_2 - \xi_1\,\text{Cos}[\xi_3] + \text{Sin}[\xi_3])\right] \tag{9}$$

Orbiting scroll

The geometry of the orbiting scroll is the same as the fixed one but is offset by π and the two scrolls are in conjugacy. Defining θ as the orbiting angle, it follows:

$$S_{me}[r_b\_, \varphi_{e0}\_, \varphi\_, r_0\_, \theta\_] := -S_{fe}[r_b, \varphi_{e0}, \varphi] - r_0 * n[\theta] \tag{10}$$

$$S_{mi}[r_b\_, \varphi_{e0}\_, \varphi\_, r_0\_, \theta\_] := -S_{fi}[r_b, \varphi_{e0}, \varphi] - r_0 * n[\theta] \tag{11}$$

The domains of definition of the internal and external involutes are, respectively, $I_e = [\varphi_{es}, \varphi_{max}]$ and $I_i = [\varphi_{is}, \varphi_{max}]$

where $r_0 = r_b(\varphi_{e0} - \varphi_{i0} + \pi)$ is the orbiting radius.

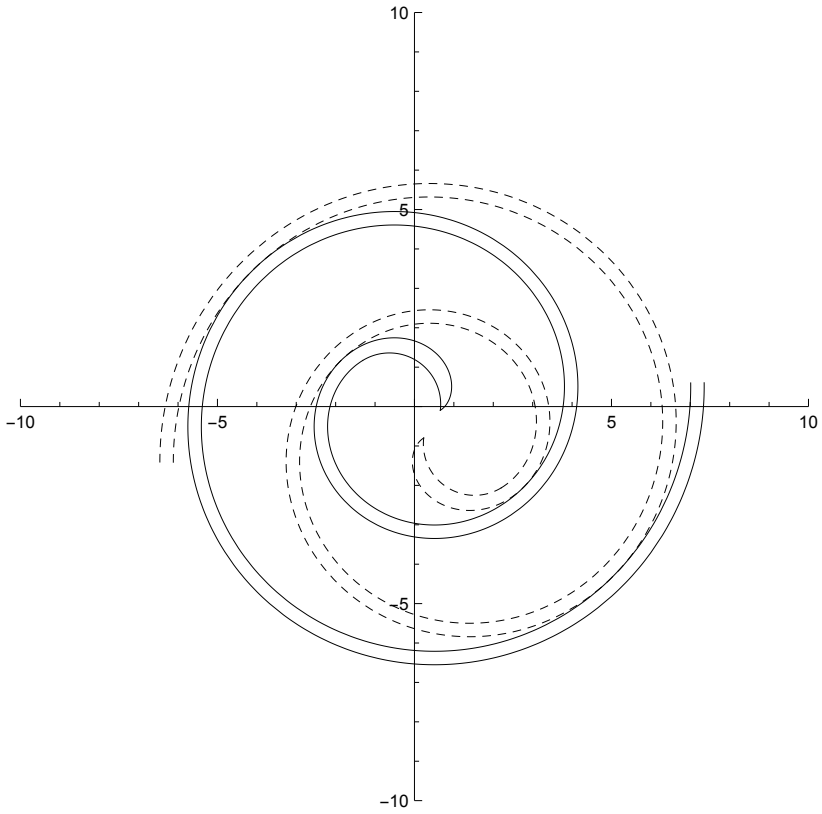

Fig 3. General Scroll reference frames

To plot the fixed and orbiting spirals we used **ParametricPlot, Show and Manipulate** instructions in *Mathematica*

Novel reference frame

In order to exploit the symmetry of the two scrolls, a novel reference frame is presented. With reference to the work of (**Gravensen and Henriksen, 2001**), the representation of the fixed scroll is given by:

$$\tilde{S}_{\text{fe}}[\varphi\_,\, \theta\_] := r_b(t[\varphi] - (\varphi - \varphi_{\text{e0}})\, n[\varphi]) + \frac{1}{2} r_0\, n[\theta] \tag{12}$$

$$\tilde{S}_{\text{fi}}[\varphi\_,\, \theta\_] := r_b(t[\varphi] - (\varphi - \varphi_{\text{i0}})\, n[\varphi]) + \frac{1}{2} r_0\, n[\theta] \tag{13}$$

The orbiting scroll is given by:

$$\tilde{S}_{\text{me}}[\varphi\_,\, \theta\_] := -\tilde{S}_{\text{fe}}[\varphi,\, \theta] \tag{14}$$

$$\tilde{S}_{\text{mi}}[\varphi\_,\, \theta\_] := -\tilde{S}_{\text{fi}}[\varphi,\, \theta] \tag{15}$$

Points of conjugacy

The kth point of conjugacy φ_{cik} at the internal involute is determined by:

$$\varphi_{\text{cik}}[\theta\_,\, \text{k}\_] := \theta + 2\,(k-1)\,\pi \tag{16}$$

The kth point of conjugacy φ_{cek} at the external involute is determined by:

$$\varphi_{\text{cek}}[\theta\_,\, \text{k}\_] := \theta - \pi + 2\,(k-1)\,\pi \tag{17}$$

For $\text{k} \in \{1 \,..\, 3\}$, we used the conditional form **Piecewise** to satisfy the existance of the points of conjugacy:

$\exists\, \varphi_{\text{cx1}}[\theta\_,\, \text{k}\_] \Longleftrightarrow \theta \geq \theta^{\text{dis}}$ **with** $\theta^{\text{dis}} = \max(\varphi_{\text{is}},\, \varphi_{\text{es}} + \pi)$

$\exists\, \varphi_{\text{cx2}}[\theta\_,\, \text{k}\_] \Longleftrightarrow \forall\, \theta$

$\exists\, \varphi_{\text{cx3}}[\theta\_,\, \text{k}\_] \Longleftrightarrow \theta \leq \theta^{\text{suc}}$ **with** $\theta^{\text{suc}} = \varphi_{\text{max}} - 4\,\pi$

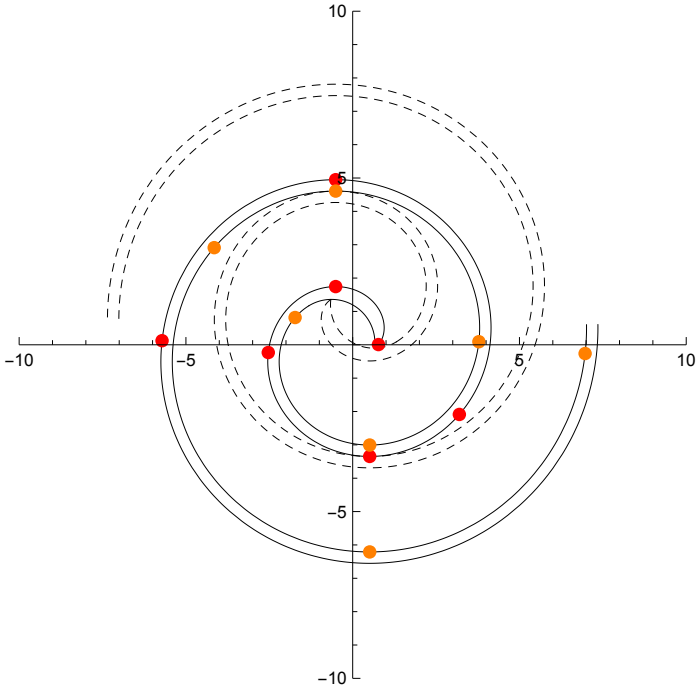

Fig 4. Point of conjugacy ● at the external fixed involute ● at the internal fixed involute

Estimation of the chamber volumes

Central chamber

The central chamber volume can be expressed as follow Blunier (2009):

$$V_0[\theta\_] := h\left(\int_{\varphi_{is}}^{\varphi_{cik}} \left\| \tilde{S}_{fi}[\varphi, \theta] \times \frac{d\tilde{S}_{fi}[\varphi, \theta]}{d\varphi} \right\| d\varphi - \frac{1}{2}\int_{\varphi_{es}}^{\varphi_{cek}} \left\| \tilde{S}_{me}[\varphi, \theta] \times \frac{d\tilde{S}_{me}[\varphi, \theta]}{d\varphi} \right\| d\varphi\right) + V_{cl}[r_b, r_c] \tag{18}$$

Where $k=\begin{cases} 1 & \text{if } \exists\ \varphi_{ci1} \\ 2 & \text{elsewhere} \end{cases}$

To take into account the two cases of k=1,2, the **Piecewise** conditional form is used.

$$V_{cl}[r_b\_, r_c\_] := h\, r_c^2\left(\pi - \text{ArcSin}\left[\frac{2\, r_b}{r_c}\right] - \frac{2\, r_b}{r_c}\right) \tag{19}$$

where $V_{cl}[r_b, r_c]$is the clearance volume of the compressor given in **Yanagisawa et al. (1990)**.

The central volume $V_0[\theta]$ can be divided into three volumes as seen in Figure 6:

$$V_{00}[\theta\_] := h\, r_c(r_c\, \beta[\theta] - (r_c - l_{ref}[\theta])\, \text{Sin}[\beta[\theta]]) \tag{20}$$

With:

$$\beta[\theta\_] := \pi - \text{ArcCos}\left[\frac{r_c - r_0 + r_0\, \text{Cos}[\theta - \theta_{ref}]}{r_c - l_{ref}[\theta]}\right] - \text{ArcSin}\left[\frac{2\, r_b}{r_c}\right] \tag{21}$$

$$l_{ref}[\theta\_] := r_c - \left(r_0^2 + (r_c - r_0)^2 + 2\, r_0(r_c - r_0)\, \text{Cos}[\theta - \theta_{ref}]\right)^{1/2} \tag{22}$$

$$V_{01}[\theta\_] := \frac{1}{2}\,(V_0[\theta] - V_{00}[\theta]) \tag{23}$$

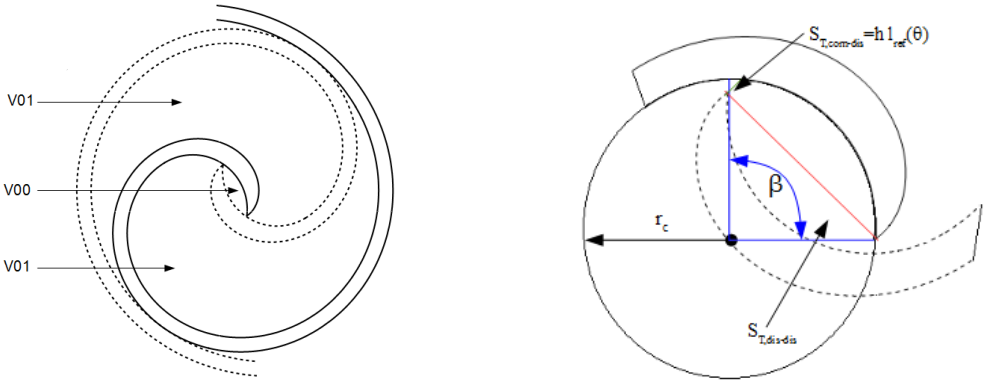

Fig 6. Volumes of the central chamber with detailed view

Suction chamber

The suction chamber volume computation is expressed as follow:

$$V_{asp}[\theta\_] := h\left(A_{aspa}[\theta] + A_{aspb}[\theta]\right) \tag{24}$$

Where:

$$A_{suca}[\theta\_] := \frac{1}{2}\int_{\varphi_{cik}}^{\varphi_{max}} \left\| \tilde{S}_{fi}[\varphi, \theta] \times \frac{d\tilde{S}_{fi}[\varphi, \theta]}{d\varphi} \right\| d\varphi - \frac{1}{2}\int_{\varphi_{cek}}^{\varphi_{max}-\pi} \left\| \tilde{S}_{me}[\varphi, \theta] \times \frac{d\tilde{S}_{me}[\varphi, \theta]}{d\varphi} \right\| d\varphi \tag{25}$$

With $k=\begin{cases} 3 & \text{if } \exists\ \varphi_{ci3} \\ 2 & \text{elsewhere} \end{cases}$

The resulting volume needs to be corrected by the area $A_{sucb}[\theta]$. This area can be calculated by the following relation:

$$A_{sucb}[\theta\_] := \frac{1}{2}\,\text{det}\left(\tilde{S}_{fi}[\varphi_{max}, \theta]\, \tilde{S}_{me}[\varphi_{max} - \pi, \theta]\right) \tag{26}$$

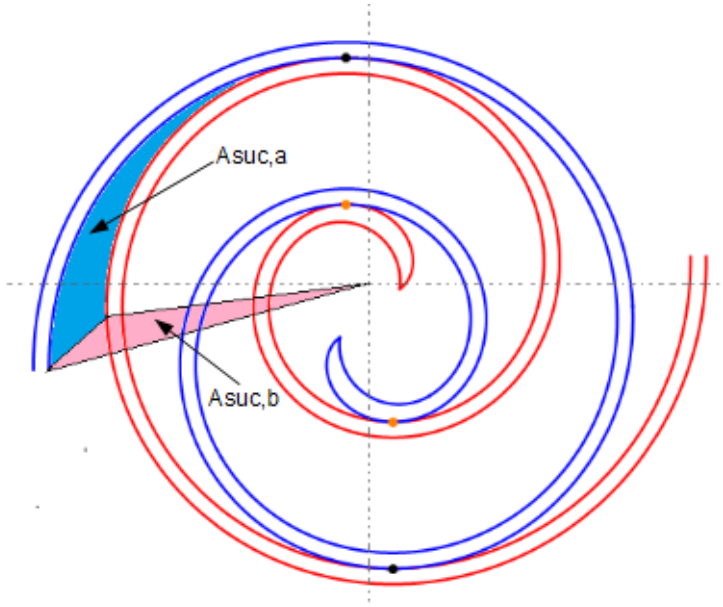

Compression chamber

The volume of the compression chamber is defined as the area enclosed by the involutes of the orbiting and the fixed scrolls between two conjugate points, multiplied by the height of the scroll.

$$V_{com}[\theta\_] := \begin{cases} \frac{h}{2}\left(\int_{\varphi_{cik}}^{\varphi_{cik+1}} \left\|\tilde{S}_{fi}[\varphi,\theta]\times\frac{d\tilde{S}_{fi}[\varphi,\theta]}{d\varphi}\right\| d\varphi - \int_{\varphi_{cek}}^{\varphi_{cek+1}} \left\|\tilde{S}_{me}[\varphi,\theta]\times\frac{d\tilde{S}_{me}[\varphi,\theta]}{d\varphi}\right\| d\varphi\right) & \text{where } k = \begin{cases} 1 & \text{if } \exists\ \varphi_{ci1} \\ 2 & \text{if } \exists\ \varphi_{ci3} \end{cases} \\ V_{01}[\theta] & \text{elsewhere} \end{cases} \quad (27)$$

Discharge chamber

The discharge chamber volume computation vs. the orbiting angle is given as:

$$V_{dis}[\theta\_] := \begin{cases} \frac{1}{2} V_0[\theta] & \text{if } \exists\ \varphi ci1 \bigvee \exists\ \varphi_{ci3} \\ \frac{1}{2} V_{00}[\theta] & \text{elsewhere} \end{cases} \quad (28)$$

the volumes of the suction, compression and discharge chambers are shown in Figure 7. Although volumes are representing through the piecewise and discontinuous functions, the compression process is continuous. Indeed, there is good continuity between suction, compression and discharge volumes as shown in the Figure 7: for example, when the suction chamber opens to compression chamber, there is good continuity of volume, pressure and temperature ensuring a continuous process.

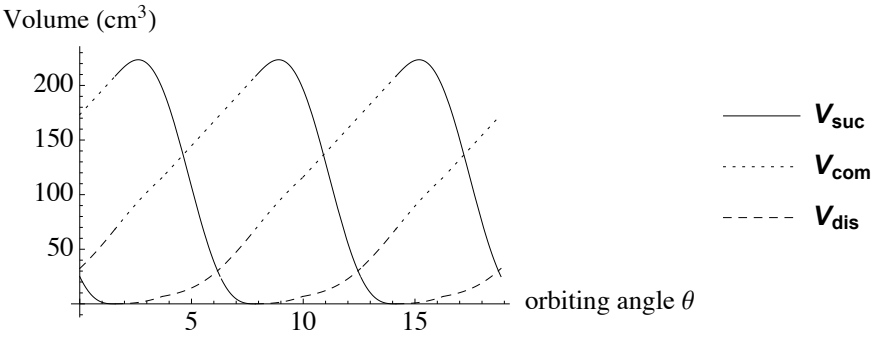

Fig 7. Chambers volumes vs. orbiting angle

Leakage computation

For a real compressor, pressures in the chambers differ from ideal pressures because leakages occur between the chambers. On the one hand the leakages increase the energy consumption (i.e., compression work) because the gas which flows from a high pressure chamber to a low pressure chamber will be compressed again. On the other hand, the leakages decrease the volumetric efficiency.
Two kinds of leakage exist in the scroll compressor:

1. Tangential (of flank) leakages (Figure 8): the gas flows through the clearance (δ_T) between the flanks of the two scrolls (in the following, the tangential leakages between the chambers x and y are noted $S_{T,x-y}$);

2. Radial leakages (Figure 9): the gas flows through the clearance (δ_R) formed between each base plate and corresponding wrap tip (in the following, the radial leakages between the chambers x and y are noted $S_{R,x-y}$).

Tangential leakages

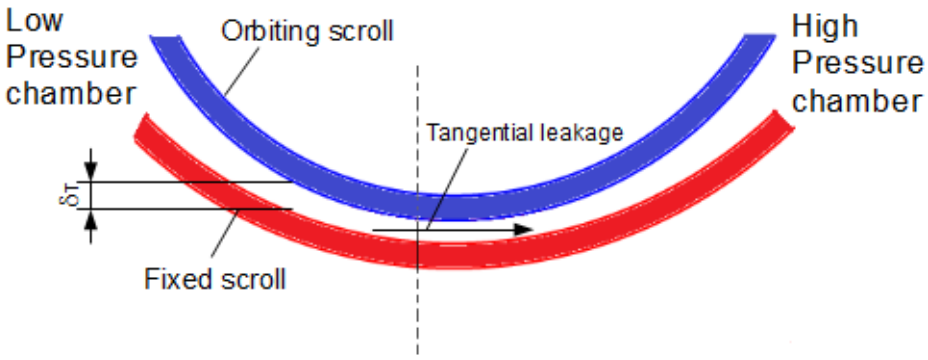

Fig 8. Tangential leakage

The suction and the discharge areas are treated as tangential leakages in the model.
When contact point exists between the chambers x and y, the leakage is computed as follow:

$$S_{T,x-y} = \delta_T\, h \tag{29}$$

where h represents the height of the spirals.

The suction leakage area is given in **Tojo et al. (1986)**:

$$S_{T,\text{amb-suc}}[\theta\_] := h(r_0(1 - \text{Cos}[\theta - \theta_{\text{suc}}] + \delta_T)) \tag{30}$$

With $\theta_{\text{suc}}=\varphi_{\max}-4\pi$

The computation of the leakage area between the compression and discharge chambers is given in **Tojo et al. (1986)**. This leakage exists if and only the compression chamber is opened in the discharge chamber (i.e., if no contact point exists between the chambers). Then, it follows:

$$S_{T,\text{com-dis}}[\theta\_] := \begin{cases} \delta_T\, h & \text{if } \exists\ \varphi_{\text{ci1}} \vee \varphi_{\text{ci3}} \\ h\, l_{\text{ref}} & \text{elsewhere} \end{cases} \tag{31}$$

The leakage areas which are between the two discharge chambers are computed as follows:

$$S_{T,\text{dis-dis}}[\theta\_] := h\left(4\, r_b{}^2\left(\varphi_{\text{es}}{}^2 - 2\,\varphi_{\text{es}}\,\varphi_{\text{e0}} + \varphi_{\text{e0}}{}^2 + 1\right) - 4\, r_b\, r_0((\varphi_{\text{es}} - \varphi_{\text{e0}})\,\text{Cos}[\theta - \varphi_{\text{es}}] + \text{Sin}[\theta - \varphi_{\text{es}}]) + r_0{}^2\right)^{\frac{1}{2}} \tag{32}$$

Radial leakages

Radial leakage is illustrated in Figure 9 between the bottom and the top plate and the scrolls. In order to calculate the leakage area from a higher pressure chamber to one with low pressure, we present in Figure 10 the different radial leakages for four positions θ.

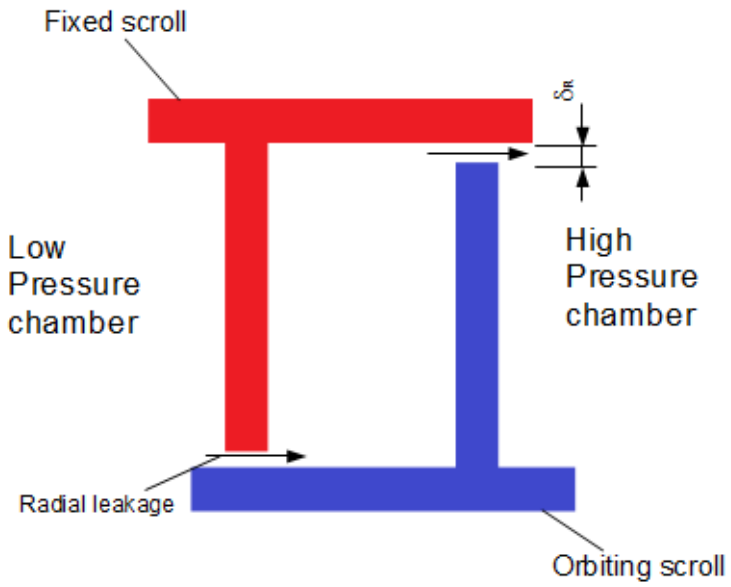

Fig 9. Radial leakage

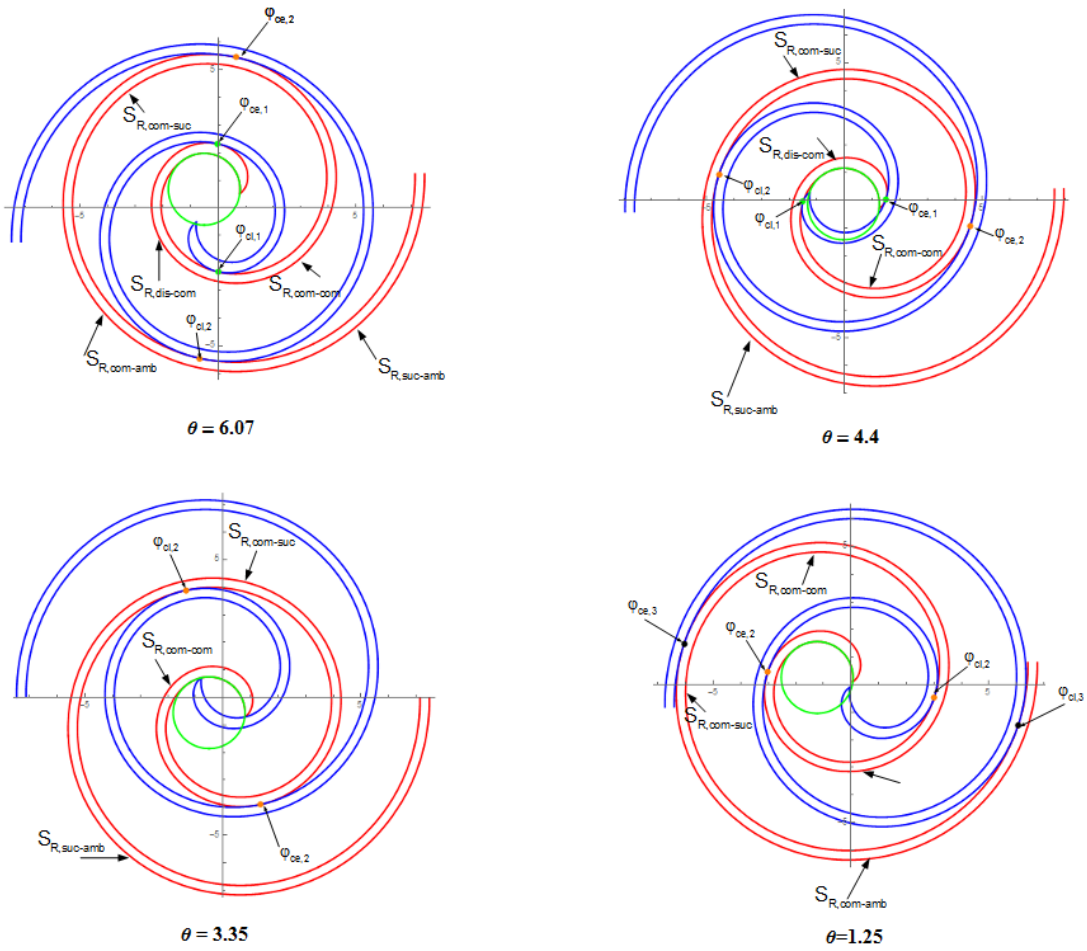

Fig 10. Radial leakages for different positions

The general expression of the radial leakage from X to Y is given by:

$$S_{R,X-Y}[\theta\_] := \delta_R \int_{\varphi 1}^{\varphi 2} \rho[\varphi]\, d\varphi \tag{33}$$

With $\rho[\varphi\_]$ is the radius of curvature of the involute, Which is expressed as:

$$\rho[\varphi\_] := r_b\left(\varphi - \frac{\varphi_{i0} + \varphi_{e0}}{2}\right) \tag{34}$$

Radial leakages between the discharge and the compression chambers are computed in the case that φ_{ce1} exists or φ_{ce3} exists. Then, it follows,

For the radial leakage from discharge to compression chamber:

$$\begin{cases} \varphi_1 = \varphi_{ce1} \text{ and } \varphi_2 = \varphi_{ci1} & \text{if } \exists\ \varphi_{ce1} \\ \varphi_1 = \varphi_{ce2} \text{ and } \varphi_2 = \varphi_{ci2} & \text{if } \exists\ \varphi_{ce3} \\ \varphi_1 = \varphi_{es} \text{ and } \varphi_2 = \varphi_{ce2} - \pi & \text{elsewhere} \end{cases}$$

The different leakages are plotted as a function of the orbiting angle θ in Figure 11.

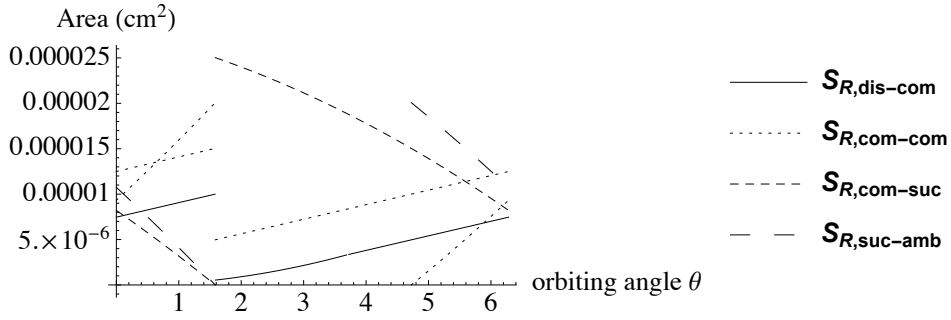

Fig 11. Radial leakages during the compression process

Thermodynamic Model

Once the geometry is known, the behaviour of each component has to be modelled.

The detailed compression process model was used to calculate the gas properties over the course of one rotation in the suction, compression, and discharge chambers as a function of the orbiting angle. The suction state of the gas is at 0.1 MPa and the discharged pressure is 1.5 MPa. The pressure as a function of the orbiting angle was plotted in figure 9 for the gas in suction chamber until the gas is discharged through the discharge chamber. Both the pre-compression phenomenon at the end of suction processand the over-compression phenomenon at the start of discharge process have been demonstrated in this figure.

The ideal working process for the scroll compressor is a suction process where the suction pocket is filled at the suction pressure, a compression process that compresses the fluid all the way to the discharge pressure, and a discharge process where the fluid is discharged at the discharge pressure. If the variation of the discharge volume and the inlet leakage of the gas can be ignored, this properties of the gas can be considered as an isentropic expansion process. This process can be described by:

$$\frac{P_2[\theta]}{P_1[\theta]} = \left(\frac{V_2[\theta]}{V_1[\theta]}\right)^{-\gamma} \tag{35}$$

Because the isentropic process does not consider leakage, Figure 12 depicts no high pressure gas flows into the working chamber.

From figure 12, it can be seen that initially the pressure in the suction chamber is equal to the suction line pressure and just before the suction chamber is entirely closed, the pressure in the suction chamber rises due to a decrease of suction pocket volume and flow resistance at the small suction port. The gas stays then in the adjacent compressor chamber until the suction chamber opens to compressor chamber and compression chamber switchs to discharge chamber where the gas keeps being discharged to the end of the cycle.

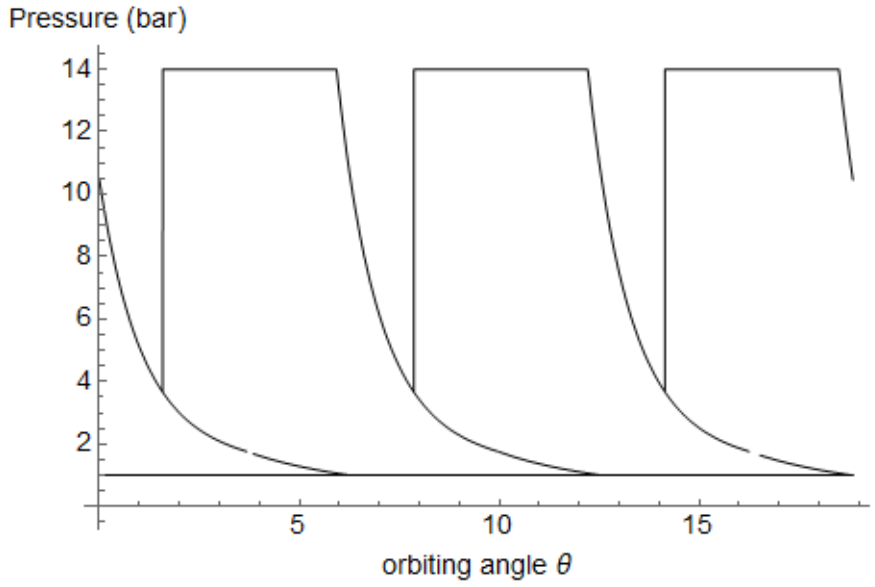

Fig 12. Pressure of the gas in the pocket as a function of the orbiting angle

Conclusion

Using *Mathematica*, this paper proposes an original way to describe the geometry of the scroll wraps in which the symmetries are easily exploited to establish a thermodynamic model of the scroll compressor: this complete geometrical description of the scroll is given using the model of Blunier (2006, 2009) where a novel reference frame is introduced and the points of conjugacy are expressed. The compression process is described in detail and the estimation of the chamber volumes and the leakages areas are given respectively. Finally an isentropic thermodynamic model of the chambers is proposed neglecting the heat transfers with the surrounding parts for successive chambers in order to predict pressure. Improvement are in progress relatively to thermodynamic evolution, description of leakage and synchronisation of these constitutive elements.

Acknowledgments

Authors would like to thank to SANDEN Manufacturing Europe for their financial support. This research has been supported by "Région de BRETAGNE-Université de RENNES1-SANDEN/Europe".

References

A. Creux, L., 1905. Rotary engine, U.S Patent 801182.

B. Yanagisawa, T., Cheng, M., Fukuta, M., Shimizu, T., 1990. Optimum operating pressure ratio for scroll compressor. In: Proceeding of the International Compressor engineering conference at Purdue, pp. 425–433.

C. Halm, N.P.,1997. Mathematical modeling of scroll compressor, Master's thesis, Herrick Lab., School of Mechanical Engineering, Purdue University.

D. Chen, Y., Halm, N.P., Groll, E.A., Braun, J.E., 2002. Mathematical modeling of scroll compressor – part I: compression process modeling. International Journal of Refrigeration 25, 731–750.

E. Lee, Y.-R., Wu, W.-F., 1995. On the profile design of a scroll compressor. International Journal of Refrigeration 18 (5), 308–317.

F. Hirano, T., Hagimoto, K., Maada, M., 1990. Scroll profiles for scroll fluid machines. MHI Technical Review 27 (1), 35–41.

G. Wang, B., Li, X., Shi, W., 2005. A general geometrical model of scroll compressors based on discretional initial angles of involute. International Journal of Refrigeration 28, 958–966.

H. Gravensen, J., Henriksen, C., Howell, P., 1998. Danfoss: Scroll Optimization, Final report. Department of Mathematics, Technical University of Denmark, Lyngby. 32nd European Study Group with Industry.

I. Gravensen, J., Henriksen, C., 2001. The geometry of the scroll compressor. Society for Industrial and Applied Mathematics 43, 113–126.

J. Blunier, B., Cirrincione, G., Miraoui, A., 2006. Novel geometrical model of scroll compressor for the analytical description of the chamber volumes. In: Proceedings of International Compressor Engineering Conference at Purdue, no. CO74.

K. Blunier, B., Cirrincione, G., Herve, Y., Miraoui, A., 2009. A new analytical and dynamical model of a scroll compressor with experimental validation. International Journal of Refrigeration 32, 874 – 891.

L. Morishita, E., Sugihara, M., Inaba, T., Nakamura, T., Works, W., 1984. Scroll compressor analytical model. In: Purdue International Compressor Engineering Conference Proceedings, pp. 487–495.

M. Nieter, J.J, 1988. Dynamics of scroll suction process. In: Purdue International Compressor Engineering Conference Proceedings, pp. 165–174.

N. Nieter, J.J., Gagne, D.P., 1992. Analytical modeling of discharge flow dynamics in scroll compressors. In: Purdue International Compressor Engineering Conference Proceedings, pp. 85–95.

O. Liu, Z., Du, G., Yu, S., Wang, M., 1992. The graphic method of modified wraps of scroll compressor. In: Proceeding of the international compressor engineering conference at Purdue, pp. 1099–1106.

P. Tojo,K., Ikegawa, M., Maeda, N., Machida, S., Shuubayashi, M. ,1986. Computer modeling of scroll compressor with self adjusting back-pressure mechanism. In: Purdue International Compressor Engineering Conference Proceedings, pp. 872–886.

Q. P. Howell, Fluid mechanical modelling of the scroll compressor, in Mathematical Modelling: Case Studies, A.Fitt and E.Cum berbatch, eds., Cambridge University Press, Cambridge, UK, 1999.